

Striatal Spreading Depolarization: Possible Implication in Levodopa-Induced Dyskinetic-Like Behavior

Antonio de Iure, PhD,^{1,2} Francesco Napolitano, PhD,^{3,4} Goichi Beck, PhD,⁵  Ana Quiroga Varela, PhD,¹ Valentina Durante, PhD,¹ Miriam Sciacaluga, PhD,¹ Petra Mazzocchetti, PhD,¹ Alfredo Megaro, BSc,¹ Michela Tantucci, PhD,¹ Antonella Cardinale, PhD,⁶ Daniela Punzo, PhD,^{7,8} Andrea Mancini, MD,¹ Cinzia Costa, PhD,¹ Veronica Ghiglieri, PhD,^{9,10} Alessandro Tozzi, PhD,^{6,9} Barbara Picconi, PhD,² Stella M. Papa, MD,^{5,11} Alessandro Usiello, PhD^{7,8} and Paolo Calabresi, MD^{1,9*}

¹Neurological Clinic, Department of Medicine, Hospital Santa Maria della Misericordia, University of Perugia, Perugia, Italy

²Laboratory of Experimental Neurophysiology, Istituto di Ricovero e Cura a Carattere Scientifico (IRCCS) San Raffaele Pisana, Rome, Italy

³Ceinge Biotechnologie Avanzate, Naples, Italy

⁴Department of Molecular Medicine and Medical Biotechnology, University of Naples "Federico II," Naples, Italy

⁵Yerkes National Primate Research Center, Emory University School of Medicine, Atlanta, Georgia, USA

⁶Department of Experimental Medicine, Section of Physiology and Biochemistry, University of Perugia, Perugia, Italy

⁷Department of Environmental, Biological and Pharmaceutical Sciences and Technologies, Second University of Naples, Caserta, Italy

⁸Istituto di Ricovero e Cura a Carattere Scientifico (IRCCS) Foundation SDN, Via Gianturco, Naples, Italy

⁹Laboratory of Neurophysiology, Santa Lucia Foundation, Istituto di Ricovero e Cura a Carattere Scientifico (IRCCS), Rome, Italy

¹⁰Department of Philosophy, Human, Social and Educational Sciences, University of Perugia, Perugia, Italy

¹¹Department of Neurology, Emory University School of Medicine, Atlanta, Georgia, USA

ABSTRACT: Objective: Spreading depolarization (SD) is a transient self-propagating wave of neuronal and glial depolarization coupled with large membrane ionic changes and a subsequent depression of neuronal activity. Spreading depolarization in the cortex is implicated in migraine, stroke, and epilepsy. Conversely, spreading depolarization in the striatum, a brain structure deeply involved in motor control and in Parkinson's disease (PD) pathophysiology, has been poorly investigated.

Methods: We characterized the participation of glutamatergic and dopaminergic transmission in the induction of striatal spreading depolarization by using a novel approach combining optical imaging, measurements of endogenous DA levels, and pharmacological and molecular analyses.

Results: We found that striatal spreading depolarization requires the concomitant activation of D1-like DA and N-methyl-D-aspartate receptors, and it is reduced in experimental PD. Chronic L-dopa treatment, inducing dyskinesia in the parkinsonian condition, increases the occurrence and speed of propagation of striatal spreading depolarization, which has a direct impact on one of the signaling pathways downstream from the activation of D1 receptors.

Conclusion: Striatal spreading depolarization might contribute to abnormal basal ganglia activity in the dyskinetic condition and represents a possible therapeutic target. © 2019 International Parkinson and Movement Disorder Society

Key Words: D1 like receptor; LIDs; Parkinson's disease; Spreading depolarization; Striatum

Spreading depolarization (SD) is a transient self-propagating wave of neuronal and glial depolarization coupled with large membrane ionic changes associated

with a depression of all neuronal activity (also referred to as spreading depression).¹ This depolarization diffuses from the point of origin to the contiguous brain tissues,

*Corresponding author: Dr. Paolo Calabresi, Neurological Clinic, Department of Medicine, University of Perugia, Hospital Santa Maria della Misericordia, 06132-S. Andrea delle Fratte, Perugia, Italy; E-mail: paolo.calabresi@unipg.it

Relevant conflicts of interests/financial disclosures: Only relevant conflicts of interest for each author that are relevant to this manuscript are reported here. All authors reported no biomedical financial interests or potential conflicts of interest. PC receives research support from Prexton and Zambon to perform preclinical investigation on drugs that may

have an effect on levodopa-induced dyskinesia but are not discussed in the text.

Received: 5 September 2018; **Revised:** 7 January 2019; **Accepted:** 14 January 2019

Published online 13 February 2019 in Wiley Online Library (wileyonlinelibrary.com). DOI: 10.1002/mds.27632

regardless of the functional and vascular territories, and although most of the studies have described SD in cortical regions, this event can also be observed in other brain areas such as the hippocampus, the striatum, and the thalamus.² SD has been associated to the pathophysiology of acute neurological disorders including migraine, ischemic stroke, and epilepsy,^{3,4} and clinical electrophysiological studies have reported cortical SD (CSD) in brain-injured patients.⁵ To date, its contribution to neurodegenerative disorders such as Parkinson's disease (PD) remains unknown.

Interestingly, CSD triggers changes in the firing pattern of striatal neurons⁶ and differentially modulates dopamine (DA) release in the ventral and dorsal striatum.⁷ This event also causes a significant increase of DA D1 receptor binding sites in the striatum,⁸ which further supports the involvement of the dopaminergic system in striatal SD (SSD). Moreover, the participation of ionotropic glutamate receptors, in particular *N*-methyl-D-aspartate (NMDA) receptors, to this phenomenon is confirmed by the block of SD by NMDA receptor antagonists.⁹⁻¹¹ The interplay between NMDA and DA signaling in this phenomenon is indicated by the effects of local application of glutamate. The activation of striatal NMDA receptors by glutamate increases extracellular DA and induces a large increase in extracellular potassium as well as a negative shift in the field potential, mimicking the ionic changes observed during SD.¹² The concomitant activation of NMDA and DA receptors in the striatum caused by the release of excitatory amino acids and DA during SD may profoundly influence the neuronal circuitry implicated in the motor control. In fact, the striatum is involved in the control of voluntary movements in both physiological and pathological conditions. This control is precisely regulated by a balanced interaction between glutamatergic and dopaminergic inputs, which is altered in PD.¹³ Dopaminergic denervation also induces morphological changes such as spine pruning in striatal spiny neurons in rat models of PD.^{14,15} Despite its potential pathophysiological role, no information is currently available on the neurochemical and molecular changes induced by SD in the striatum as well as on the distinct role of endogenous DA and glutamate in the induction and propagation of this event.

Here, we have investigated the participation of the neurotransmitters DA and glutamate in the induction of SSD using a novel approach that combines optical imaging, measurements of endogenous DA levels, and molecular analysis. Surprisingly, we also found that, although SSD is dramatically reduced in the striatum of parkinsonian animals, chronic L-dopa treatment leading to the development of dyskinesias enhances the occurrence and the speed of propagation of this event by modulating a specific signaling pathway downstream from the activation of D1 receptors.

Materials and Methods

Ethic Statement on Animal Use

All *in vitro* and behavioral procedures performed in Wistar rats were conducted in conformity with the European Communities Council Directive 2010/63/EU in accordance with the protocol (no. 1013/2015-PR) approved by the Animal Care and Use Committee at the University of Perugia (Perugia, Italy).

Preparation and Maintenance of Corticostriatal Slices

The slices were maintained as previously described in Krebs's solution, bubbled with a 95% oxygen (O₂)/5% carbon dioxide (CO₂) (vol/vol) gas mixture at room temperature.^{11,16} SSD was induced in the presence of a magnesium (Mg²⁺)-free Krebs's solution in all experiments if not differently specified.

Imaging of Striatal Spreading Depression

Optical imaging has been selected to study SSD because this technique offers good spatial and temporal resolution simultaneously, making it ideal for studying pathophysiological events during SSD. An intrinsic optical signal (IOS) is produced by changes in the light transmittance of brain slice tissue as previously described.¹¹

Electrophysiology

Electrophysiological changes produced by potassium chloride (KCl)-induced SSD in striatal slices were measured in some experimental groups by analyzing the discontinuous current (DC) potential shifts recorded, simultaneously to the IOS signal, prior and following the KCl application.

Constant Potential Amperometry

To monitor DA during SSD we used constant potential amperometry with a carbon fiber recording electrode (CF10, active surface 30 μm in diameter and 100 μm long; World Precision Instruments, Friedberg, Germany) gently positioned into the dorsal striatum to a depth of 100 to 150 μm near the region of interest.¹⁷

6-Hydroxydopamine (6-OHDA) DA-Denervation and Abnormal Involuntary Movements (AIMs)

In brief, the rats were deeply anesthetized and unilaterally injected with 6-hydroxydopamine (6-OHDA) or with saline only (sham-operated rats) into the medial forebrain bundle as previously reported.^{16,18} L-dopa treatment and Abnormal Involuntary Movements (AIMs) score were performed as previously published.^{16,19}

Western Blotting

Striatal rat slices were sonicated in 1% sodium dodecyl sulfate (SDS) and boiled for 10 minutes. The effectiveness of this extraction procedure in preventing protein phosphorylation and dephosphorylation, hence ensuring that the level of phosphoproteins measured *ex vivo* reflects the *in vivo* situation, has been previously tested.²⁰

All Material and Methods and statistical details are available in the online Supporting Information.

Results

Physiological Characterization of SD in the Corticostriatal Slice

Single corticostriatal rat slices were placed in a recording chamber in a continuously flowing oxygenated Krebs' solution and visualized by means of an upright microscope equipped with a 2× objective and a charge-coupled device (CCD) camera.¹¹ SSD was induced by perfusing the slice with 26 mM potassium chloride (KCl) for 4 minutes. Optical imaging of the intrinsic signals is obtained by measuring intrinsic activity-related changes in tissue reflectance. Functional changes result in intrinsic tissue reflectance changes that are used to map functional brain activity.²¹ Thus, an IOS provides insights into brain activity and allows the analysis of SD in the submerged slice. SSD was characterized by a propagation of light transmittance through the entire area of the corticostriatal slice (Fig. 1A) and was measured as IOS changes characterized by a biphasic transient increase consisting of an early IOS peak followed by a delayed long-lasting phase (Fig. 1B; time course of a representative SSD trace). SSD was also induced by local puff application of 2 mol/Lt KCl (*n* = 5; Fig. S1). In some experiments, IOS acquisitions were paralleled by simultaneous measurements of DC potentials (Figs. 1B, 2C and Fig. S4B). The analysis of the time course of DC potentials showed that about 4 minutes following KCl application, a transient rapid negative shift of DC potential, followed by a delayed negative phase, was induced. Interestingly, the first early negative DC peak temporally corresponded to the early peak of IOS. The measure of striatal projection neuron (SPN) membrane potential showed that KCl application was able to induce a rapid membrane depolarization after a few seconds from the KCl onset and that this shift returned to baseline at the washout (Fig. 1B). The time to onset of SSD was around 3 minutes in control conditions; a minute was necessary to observe the spreading of the IOS change through the entire striatal slice. A single IOS change terminated within 15 minutes from the onset of KCl application. Usually, 20 minutes between each KCl application were required to generate SSD episodes of a similar extent (Fig. 1C-E). SSD was highly reproducible in a magnesium-free solution (Fig. 1F), whereas in the

presence of 1.2 mM external magnesium, SSD was observed only in 60% and in 40% of the slices, respectively, for the 1st and 2nd episodes (Fig. 1F).

Effect of Ionotropic Glutamate Receptor Antagonists on SSD

The 100% occurrence of SSD in the magnesium-free Krebs' solution suggests a critical role of the NMDA glutamate receptor in this phenomenon. We thus investigated whether the activation of ionotropic glutamate receptors was required for the initiation and propagation of SSD because the involvement of these receptors has been described for CSD.^{3,11} To address this issue, a first induction of SSD was obtained in a group of slices perfused with a magnesium-free solution (Fig. 2A,B). After the first episode (predrug), 50 μM L-aminophosphonovaleate (L-APV), a NMDA glutamate receptor antagonist, was bath applied for 10 minutes and then coapplied with KCl. In this condition, the propagation of SSD was completely blocked, with IOS intensity dramatically reduced for both the early peak and the delayed phase (Fig. 2B, right panel, *P* < .001). Interestingly, SSD was also present in the decorticated slices, suggesting that this phenomenon may arise and diffuse within the striatum, whereas the cortex is not necessarily involved (Fig. S2A). Moreover, L-APV also significantly reduced SSD in the decorticated slices (Fig. 2C, *P* < .05), clearly indicating that NMDA receptors, causally implicated in this phenomenon, are located within the striatum. Conversely, pretreatment of the slices with 6-cyano-7-nitroquinoxaline-2,3-dione (CNQX) (10 μM), an α-amino-3-hydroxy-5-methyl-4-isoxazolepropionic acid (AMPA) glutamate receptor antagonist, also applied for 10 minutes, failed to affect SSD (Fig. 2D,E). These data suggest that activation of NMDA, but not AMPA receptors, is required for SSD. Transient increases of extracellular glutamate and intracellular calcium concentrations²² activate extracellular signal-regulated kinase (ERK) signaling.²³ Thus, here we evaluated the activation state of this signaling pathway in rat striatal slices subjected to SSD. Consistent with previous observations in the cortex,²⁴ our data confirmed a significant increase of striatal phosphorylation levels of ERK (Fig. 2F).

SSD Is Blocked by D1-Like but not D2-Like DA Receptor Antagonists

Considering the reported changes of dopaminergic transmission observed during SD,^{7,8} we investigated the potential involvement of D1-like and D2-like receptors during SSD. Fifteen minutes following a first episode of SSD in the control condition, we bath incubated the slices for an additional 10 minutes with 10 μM SCH 23390, a D1 receptor antagonist (Fig. 3A). SCH 23390 blocked the propagation of SSD, reducing the IOS amplitudes (Fig. 3B, *P* < .001). We also investigated the

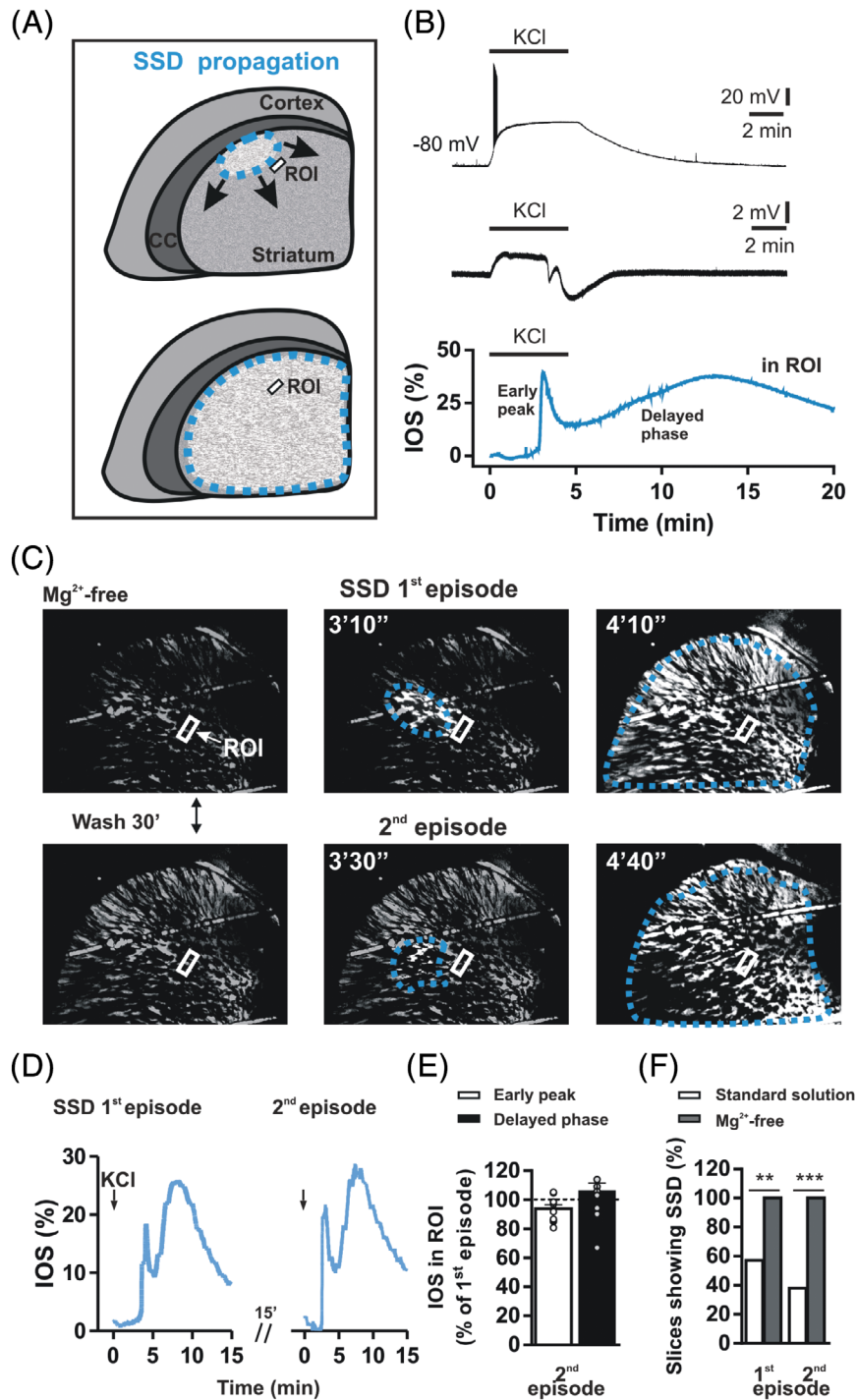
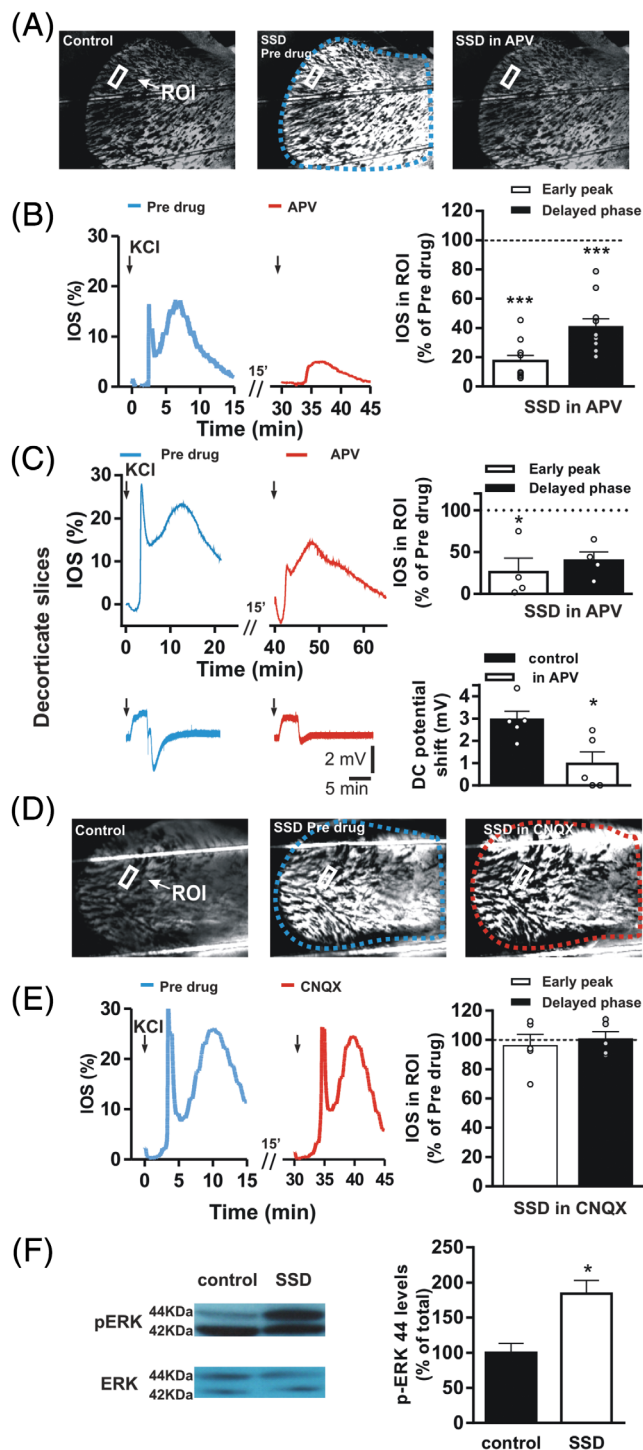


FIG. 1. Spreading depolarization originating within the nucleus striatum in rat corticostriatal slice. **(A)** Drawing of a coronal corticostriatal rat slice showing the propagation of striatal spreading depolarization (SSD) that originates within striatal tissue (left) and diffuses to the whole striatum. **(B)** Representative traces showing the change of the resting membrane potential of a striatal spiny projection neuron (top), of the striatal DC potential (middle) and of the intrinsic optical signal (IOS) drawn in a region of interest (ROI; bottom) following a 4-minute application of 26 mM potassium chloride (KCl) to a corticostriatal slice maintained in a standard Krebs's solution. **(C)** Images of a representative rat corticostriatal slice, maintained in a magnesium-free Krebs's solution, showing 2 consecutive SSD episodes propagating over time. **(D)** Graph showing the IOS changes measured from the slice presented in **C** during the first and second SSD episodes induced by KCl application (arrow). Note the typical biphasic IOS change associated to a KCl-induced SSD. **(E)** Histogram showing the early peak and delayed phase amplitudes of IOS changes during the second SSD episode with respect to the first SSD episode (dotted line, control in predrug condition; $n = 11$ slices for each experimental group; early peak, % of 1st episode, $95.57 \pm 2.34\%$, $t_{10} = 1.89$, $P > .05$; delayed peak, % of 1st episode, $106.0 \pm 5.58\%$, $t_{10} = 1.082$, $P > .05$, paired Student's t test). **(F)** Histogram showing the percentage of striatal slices presenting SSD following KCl application when maintained in a standard Krebs's solution (standard solution, 60%, $n = 12$ of 21 slices and 40%, $n = 8$ of 21 slices) or in a magnesium-free solution (Mg²⁺-free, $n = 15$ of 15 slices). ** $P < .01$, *** $P < .001$, chi-square test. CC, corpus callosum. [Color figure can be viewed at wileyonlinelibrary.com]

possible role of D2 receptors by inducing SSD in a group of slices before and after the incubation with 3 μ M L-sulpiride, a D2-like receptor antagonist (Fig. 3C,D). We found that the antagonism of D2 receptors had no effect on SSD because IOS was not affected by this treatment (Fig. 3C,D, right panel). Overall, these pharmacological observations point to a major involvement of D1-like receptors on the onset and diffusion of SSD.



The DA D1 receptors are positively coupled to adenosine 3',5'-cyclic monophosphate (cAMP) accumulation^{25,26} that, in turn, activates the cAMP-dependent protein kinase (PKA) pathway. We then investigated the influence of SSD on the state of striatal adenosine 3',5'-cyclic monophosphate (cAMP)/protein kinase A (PKA) activation by evaluating the phosphorylation levels of glutamate Ampa receptor 1 (GluA1) at residue (pGluA1), a selective PKA substrate.²⁷ Our data showed for the first time a robust influence of SSD on the striatal increase of pGluA1 levels in vehicle-treated slices (Fig. 3E, $P < .001$). Consistent with these findings, we also showed that 10 μ M of the D1 receptor agonist SKF 38393 induced an increase of striatal cAMP/PKA activity under the SSD protocol application not found in slices incubated with 10 μ M SCH 23390 (Fig. 3E, $P < .05$).

Finally, to assess the functional contribution of an intact striatal cAMP/PKA pathway to the development of SSD, we tested the effect of the PKA inhibitor H89 under the SSD protocol. Interestingly, consistent with a causal role of this signaling pathway in triggering SSD, H89

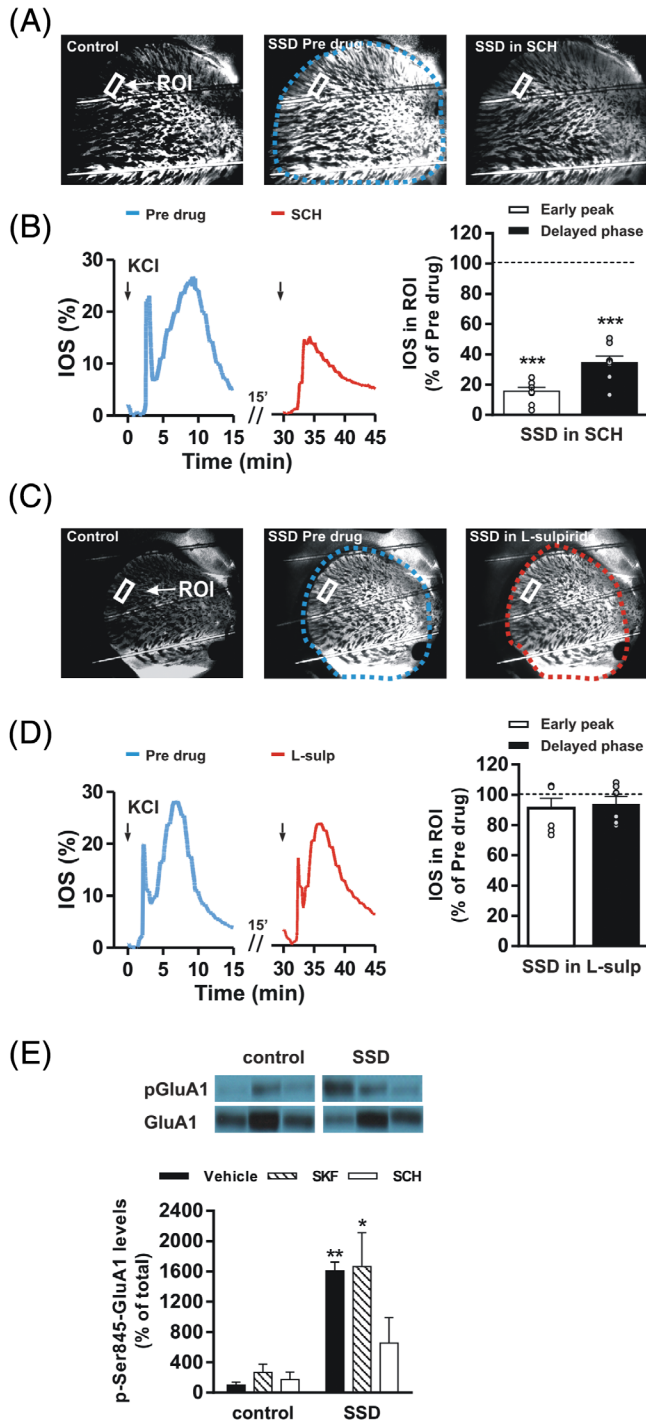
FIG. 2. Striatal spreading depolarization (SSD) is prevented by *N*-methyl-D-aspartate (NMDA), but not α -amino-3-hydroxy-5-methyl-4-isoxazolepropionic acid (AMPA), receptor antagonism and triggers phosphorylation of extracellular signal-regulated kinase (ERK). **(A)** Images of a cortico-striatal slice in control conditions (left) during a potassium chloride (KCl)-induced SSD (middle) and following a second episode of SSD induced by a KCl application in the presence of the NMDA receptor antagonist L-aminophosphonovalerate (L-APV). **(B)** The graph on the left shows the intrinsic optical signal (IOS) changes, measured in the region of interest (ROI) of the slice presented in **A** during the first SSD episode (predrug condition) and during the second SSD episode recorded in the presence of L-APV. The histogram shows the IOS peaks amplitudes during the second episode of SSD induced in the presence of L-APV in respect to the first SSD episode (control in pre-drug condition; early peak, predrug vs APV, $n = 11$ slices for both, $17.32 \pm 3.88\%$, $t_{10} = 21.27$, $***P < .001$; delayed phase, $n = 11$ for both, $40.85 \pm 5.38\%$, $t_{10} = 10.98$, $***P < .001$, paired Student's *t* test). **(C)** Traces on the left show striatal IOS (top) and DC potential (bottom) recordings during a first SSD episode (control) and during a second episode in the presence of L-APV in a decorticated slice. Histogram on the right show the IOS peaks amplitudes (top) and discontinuous current (DC) potential shifts (bottom) during SSD induced in the presence of L-APV in decorticated slices. (IOS: early peak, predrug vs APV, $n = 4$ slices for both, $26.09 \pm 16.77\%$, $t_6 = 2.8$, $*P < .05$; delayed phase, $n = 4$ for both, $39.9 \pm 10.41\%$, $P > .05$; DC potential shift, predrug vs APV, $n = 5$ slices, $t_4 = 2.8$, $*P < .05$, paired Student's *t* test). **(D)** Images of a cortico-striatal slice in control conditions (left) during a KCl-induced SSD (middle) and following a second episode of SSD in the presence of the AMPA receptor antagonist 6-cyano-7-nitroquinoxaline-2,3-dione (CNQX). **(E)** The graph on the left shows the IOS changes, measured in the ROI of the slice in **D**, during SSD induced in predrug condition and during the second SSD episode induced in the presence of CNQX. The histogram shows the IOS peak amplitudes during the second episode of SSD induced in the presence of CNQX in respect to the first SSD episode (control in predrug condition; early peak, predrug, $n = 6$ slices, vs CNQX, $n = 5$ slices, $95.91 \pm 7.72\%$, $t_4 = 0.529$, $P > .05$; delayed phase, predrug vs CNQX, $n = 5$ slices for both, $100.6 \pm 5.03\%$, $t_4 = 0.109$, $P > .05$; paired Student's *t* test). **(F)** Striatal ERK phosphorylation levels in rat slices following SSD ($n = 3$ slices for both groups, control, $100.0 \pm 13.31\%$ vs SSD, 184.1 ± 18.94 , $t_4 = 3.63$, $*P < .05$, unpaired Student's *t* test). All data are expressed as mean \pm standard error. SSD is induced in a magnesium-free solution. [Color figure can be viewed at wileyonlinelibrary.com]

blocked the onset and the diffusion of this phenomenon in the 80% of the striatal slices analyzed (Fig. S2B).

SSD Induces H3-Dependent Chromatin Modifications and Activates *c-Fos* and *Npas4* Gene Expression

Herein we addressed the question of whether SSD might also exert nuclear effects influencing H3 histone modifications. To this aim, we first observed that SSD

induced a higher phosphorylation state of the striatal H3 histone at Ser10 in rat slices (Fig. S3A) when compared with controls ($P < .01$). We then analyzed the H3-dependent gene expression levels of the immediate early genes, such as *c-Fos* and *Npas4* mRNAs,²⁸ under SSD protocol. Consistent with a previous study performed in the cortex, quantitative real-time PCR analysis carried out 60 minutes after the SSD protocol clearly showed a significant striatal increase of both *c-Fos* and *Npas4* mRNA levels in rat slices when compared with controls (Fig. S3B, $P < .05$).



DA Release Is Associated With SSD Propagation

SSD is accompanied by the release and diffusion of several chemical mediators that affect different receptors, possibly playing important roles in this phenomenon.^{3,7} We investigated whether DA overflow could be evoked in the striatal slice of control animals during SSD. To monitor the KCl-evoked DA release, we used a carbon fiber electrode connected to a picoamperometer/potentiostat.¹⁷ The electrode, positioned in the striatal slice, was used to apply a voltage and to measure the currents (Fig. 4A). For the imaging analysis, we located a region of interest in the close proximity of the tip of the carbon fiber electrode to observe IOS changes

FIG. 3. Striatal spreading depolarization (SSD) is prevented by D1, but not D2, DA receptor antagonism and is associated with phosphorylation of the α -amino-3-hydroxy-5-methyl-4-isoxazolepropionic acid (AMPA) GluA1 subunit. **(A)** Images of a corticostriatal slice in control conditions (left) during a potassium chloride (KCl)-induced SSD (middle) and following a second episode of SSD in the presence of the D1 DA receptor antagonist SCH 23390. **(B)** The graph on the left shows the intrinsic optical signal (IOS) changes, measured in the region of interest (ROI) of the slice presented in **A**, during the first (predrug condition) and the second SSD episode recorded in the presence of SCH 23390. The histogram shows the IOS peak amplitudes during the second SSD episode induced in the presence of SCH 23390 in respect to the first SSD episode (control in predrug condition; $n = 8$ slices for both groups, early peak, predrug vs SCH, $15.58 \pm 2.65\%$, $t_7 = 31.86$, $***P < .001$; delayed phase, predrug, $n = 7$ slices, vs SCH, $n = 8$ slices, $34.61 \pm 4.18\%$, $t_6 = 18.79$, $***P < .001$; paired Student's t test). **(C)** Images of a corticostriatal slice in control conditions (left) during a KCl-induced SSD (middle) and following a second episode of SSD in the presence of the D2 DA receptor antagonist L-sulpiride (L-sulp). **(D)** The graph on the left shows the IOS changes measured in the ROI of the slice presented in **C** during the first SSD episode (predrug condition) and the second SSD episode recorded in the presence of L-sulpiride. The histogram shows the IOS peak amplitudes during the second SSD episode induced in the presence of L-sulpiride with respect to the first SSD episode (dotted line, control in predrug condition; $n = 6$ slices for all groups, early peak, predrug vs L-sulp, $91.14 \pm 6.60\%$, $t_5 = 1.34$, $P > .05$; delayed phase, predrug vs L-sulp, $93.66 \pm 5.21\%$, $t_5 = 1.21$, $P > .05$; paired Student's t test). **(E)** Striatal GluA1 phosphorylation levels at Ser845 residue in rat slices undergoing SSD, under both basal condition (vehicle; $n = 3$ for each experimental group; 2-way analysis of variance, SSD effect, $F_{1,12} = 32.50$, $P < .0001$; vehicle CTR vs vehicle SSD, $t_4 = 12.32$, $***P = .0002$, unpaired Student's t test) and following a bath application of $10 \mu\text{M}$ SKF 38393 (SSD, $t_4 = 3.47$, $*P = .0256$, unpaired Student's t test) or $10 \mu\text{M}$ SCH 23390 (SSD, $t_4 = 0.66$, $P = .5450$). SSD is induced in a magnesium-free solution. All data are expressed as mean \pm standard error. [Color figure can be viewed at wileyonlinelibrary.com]

in relation to the DA release. During the progression of SSD, the IOS early peak was accompanied by a release of DA. The peak amplitude of DA release during the 1st episode was 0.85 ± 0.18 nA in control conditions (Fig. 4B). Two consecutive applications of KCl were able to induce consecutive episodes of SSD with similar DA peaks (Fig. 4C, right panel).

SSD Is Blocked by DA Denervation and Restored by D1 Receptor Activation

To better evaluate the influence of dopaminergic tone on the modulation of SSD, we used slices from 6-OHDA-lesioned rats to induce SSD in the absence of endogenous DA. This animal model of PD is characterized by near total loss of dopaminergic neurons in the

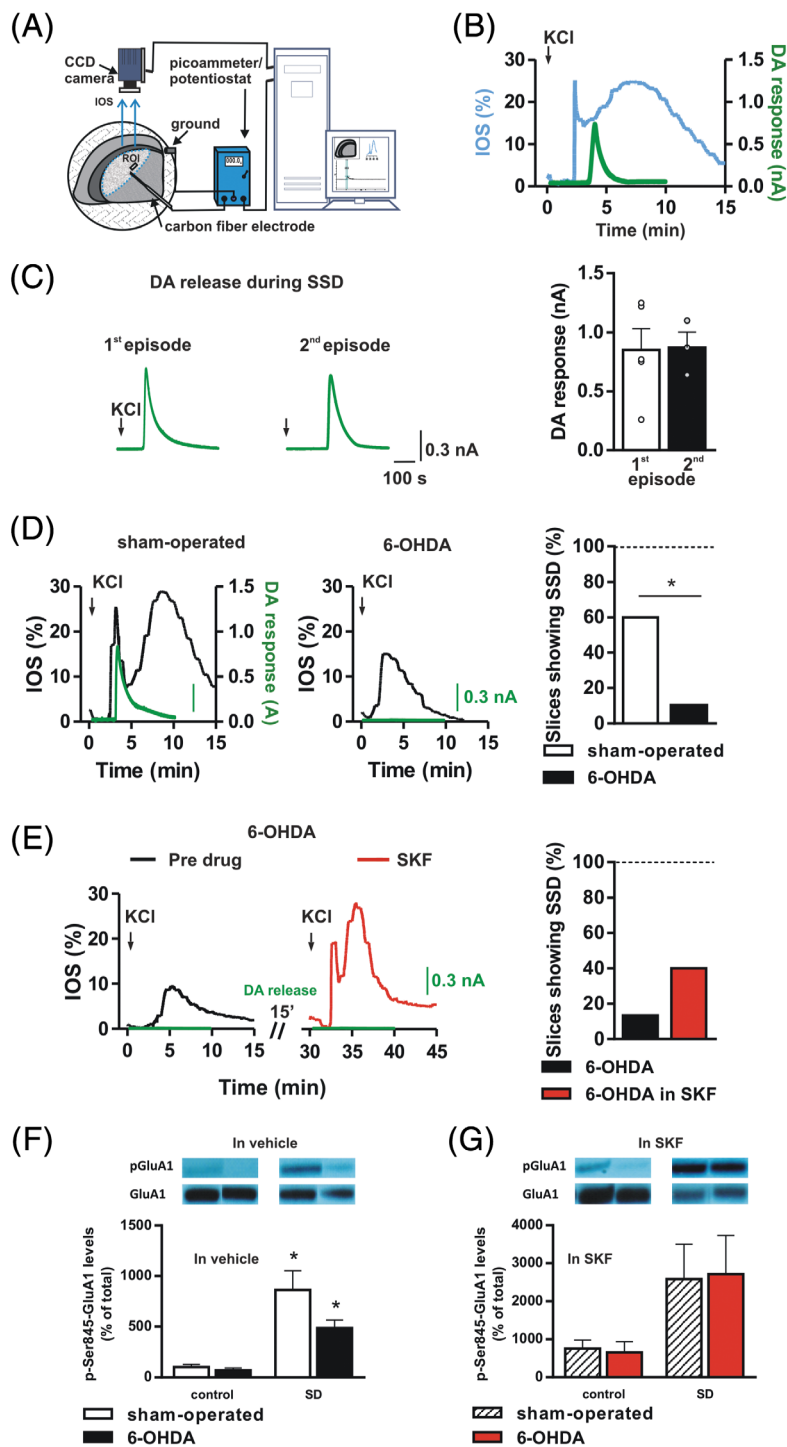


FIGURE 4. Legend on next page.

substantia nigra.¹⁶ In physiological condition, nigrostriatal fibers project to the striatum to release DA. Although in sham-operated rats we observed SSD induction in 60% of the slices in the physiological solution (1.2 mM external magnesium; $n = 12$ of 20 slices), in slices from the 6-OHDA-lesioned animals, SSD was observed only in 10% of the cases ($n = 2$ of 20 slices; Fig. 4D, right panel, $P < .05$). In these experiments, we also measured the DA levels during SSD. As expected, slices from 6-OHDA animals had no detectable DA release after KCl perfusion (Fig. 4D), whereas those obtained from sham-operated rats showed a DA release (green trace) similar to that observed in the control condition (Fig. 4D compared with DA release green trace showed in Fig. 4B).

We then incubated for 10 minutes striatal slices from 6-OHDA rats with 10 μM of the D1 receptor agonist SKF 38393, observing that drug incubation restored SSD in 40% of the DA-depleted slices ($n = 6$ of 15 slices incubated with SKF 38393), whereas in the absence of DA D1 receptor agonist, SSD was observed only in 13.3% of the slices recorded from 6-OHDA rats ($n = 2$ of 15 slices; Fig. 4E, right panel). We then analyzed the effect of SSD on the striatal cAMP/PKA signaling in unilaterally 6-OHDA-denervated rat slices. Interestingly, we found that in both the sham-operated and 6-OHDA rats, SSD triggered an overall increase of pGluA1 levels (Fig. 4F, $P < .05$), although a slight 50% downward trend in SSD-dependent increase of cAMP/PKA activity was observed in the 6-OHDA-lesioned slices. Finally, to further confirm that SSD onset and diffusion depend on intact striatal D1 receptor activation, we evaluated striatal pGluA1 levels in DA-denervated rat slices that showed SSD treated with 10 μM SKF 38393. Our data show that the D1 receptor agonist was able to rescue the striatal cAMP/PKA reduction found in untreated lesioned slices (Fig. 4G, $P < .05$).

Dyskinetic Rats Show an Increased Expression and Propagation of SSD

Striatal slices were obtained from different experimental groups of 6-OHDA rats in 2 different conditions. In the first group, L-dopa was administered subchronically (intraperitoneal, i.p. injections) for 3 days, whereas the other group received a chronic treatment lasting 15 days. As previously reported,^{16,19,29} chronic L-dopa treatment induced the appearance of dyskinetic movements in about half of the chronically L-dopa-treated 6-OHDA rats, whereas the remaining animals showed a beneficial response to this drug. This differential pharmacological response to chronic L-dopa treatment allowed us to identify these 2 additional groups also in our experimental parkinsonian animals. We then investigated the features of SSD in slices obtained from these 3 experimental groups (6-OHDA plus L-dopa [3 days]; 6-OHDA plus L-dopa [15 days]; non dyskinetic, 6-OHDA plus L-dopa [15 days] dyskinetic; Fig. 5). The percentage of slices showing SSD was 75% in DA-denervated rats receiving subchronic treatment ($n = 12$ of 16 slices), 70% in chronically L-dopa-treated non dyskinetic rats ($n = 7$ of 10 slices), and 100% in chronically L-dopa-treated dyskinetic rats ($n = 14$ of 14 slices; Fig. 5A). Surprisingly, the DA level that was measured using amperometry in the different 6-OHDA-lesioned experimental groups treated with L-dopa was similar (Fig. 5B). DA denervation results in the absence of DA content when measured from the slices of 6-OHDA rats compared with sham-operated animals. The peak amplitude of DA release, recorded in the slices of the sham-operated rats (0.69 ± 0.063 nA), was significantly different from the DA peak amplitude in the slices of 6-OHDA animals that received 3 days of L-dopa treatment as well as from the non dyskinetic and from dyskinetic rats (Fig. 5B). Interestingly, L-dopa treatment

FIG. 4. Striatal spreading depolarization (SSD) is dependent on striatal DA levels stimulating the D1 receptor-mediated signaling pathway. **(A)** Representation of the acquisition system for the combined intrinsic optical signal (IOS) and amperometric detection in rat corticostriatal slices. The IOS emitted from the slice is acquired by a charge-coupled device (CCD) camera and transferred to a personal computer. Amperometric currents are detected by a carbon fiber electrode connected to a potentiostat also interfaced to the personal computer. A potassium chloride (KCl) application delivered by a perfusion system can trigger a SSD episode and DA release in the slice preparation. **(B)** Graph showing the superimposed time courses of the percentage IOS (left y axis) and the DA concentration (right y axis) changes associated to a KCl-induced SSD. **(C)** Traces of amperometric transient currents showing changes in DA concentration following KCl applications during 2 consecutive SSD episodes. The histogram shows reproducible DA concentration increases associated to first and second KCl-induced SSD episodes (1st episode, $n = 5$, 0.85 ± 0.18 nA vs 2nd episode, $n = 3$, 0.87 ± 0.13 nA, $t_6 = 0.076$, $P > .05$, unpaired Student's t test). **(D)** Graphs showing the superimposed time courses of the percentage IOS and the DA concentration changes associated with a KCl-induced SSD in a slice of a sham-operated rat and of a 6-Hydroxydopamine (6-OHDA) DA-denervated animal. Histogram showing the percentage of slices of sham-operated and 6-OHDA rats presenting SSD ($*P < .05$, chi-square test). **(E)** Graph showing the superimposed time courses of the percentage IOS and the DA concentration changes during the first SSD episode (predrug condition) and during the second SSD episode recorded in the presence of SKF 38393 in a slice of a 6-OHDA DA-denervated rat. Histogram showing the percentage of slices of 6-OHDA rats presenting SSD in the presence and absence of the D1 receptor agonist SKF 38393. **(F, G)** Glutamate Ampa Receptor 1A (GluA1) GluA1 phosphorylation levels at Ser845 residue in the striatum of 6-OHDA-lesioned rat slices following SSD under both basal conditions (**F**; $n = 3$ for all of the experimental groups; 2-way analysis of variance; SSD effect, $F_{1,8} = 31.90$, $*P = .0005$) and on bath application of 10 μM SKF 38393 (**G**; $n = 3$ for all of the experimental groups; 2-way analysis of variance; SSD effect, $F_{1,8} = 7.494$, $P = .0255$); **(G)**. SSD is induced in a standard Krebs's solution. All data are expressed as mean \pm standard error. $*P < .05$. [Color figure can be viewed at wileyonlinelibrary.com]

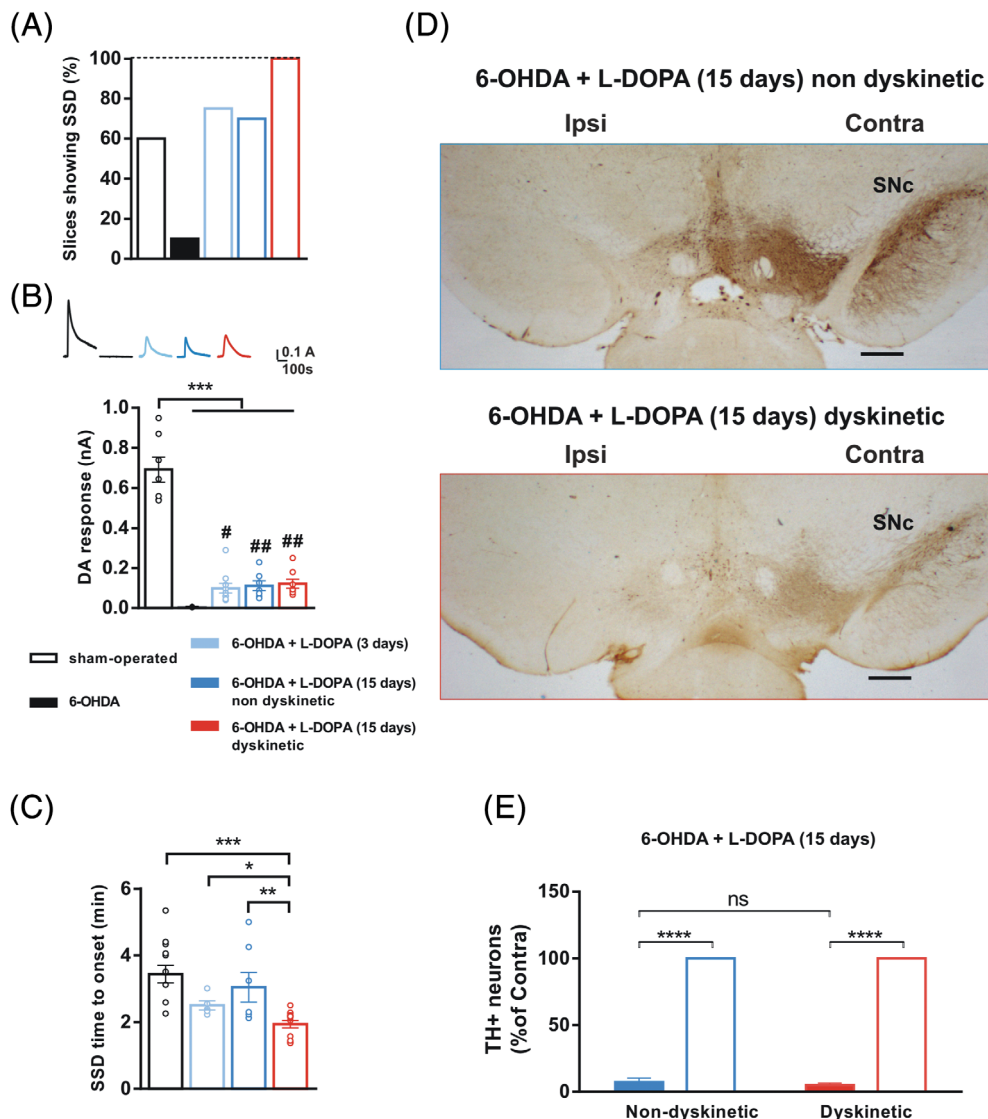


FIG. 5. Striatal spreading depolarization (SSD) and DA levels in dyskinetic and non-dyskinetic rats. **(A)** Histogram showing the percentage of corticostriatal slices presenting SSD in different experimental groups of sham-operated, 6-OHDA-denervated, and L-dopa-treated 6-OHDA (dyskinetic and non-dyskinetic) rats. **(B)** Histogram and representative traces of the amperometric striatal DA peak currents measured in corticostriatal slices of the different animal groups used for SSD measure ($n = 5$ 6-OHDA vs $n = 7$ sham operated, $t_{10} = 9.083$, $***P < .001$; $n = 10$ 6-OHDA plus L-dopa [3 days] vs $n = 7$ 6-OHDA plus L-dopa [15 days] non-dyskinetic, $t_{15} = 0.37$, $P > .05$; 6-OHDA plus L-dopa [3 days] vs $n = 8$ 6-OHDA plus L-dopa [15 days] dyskinetic, $t_{16} = 0.65$, $P > .05$; unpaired Student's t test). DA peak amplitude of DA release in the slices of sham-operated rats versus slices of sham-operated rats treated with L-dopa for 3 or 15 days (dyskinetic and non-dyskinetic; sham vs dyskinetic, $t_{25} = 5.32$, $***P < .001$; non-dyskinetic vs dyskinetic, $t_{19} = 3.22$, $**P < .01$, unpaired Student's t test) as well as from non-dyskinetic (15 days non-dyskinetic; 0.109 ± 0.022 nA, $t_{12} = 8.57$, $***P < .001$, unpaired Student's t test) and from dyskinetic rats (15 days dyskinetic; 0.127 ± 0.021 nA, $t_{13} = 9.021$, $***P < .001$, unpaired Student's t test; 6-OHDA, $t_{13} = 2.76$, vs 3 days, $t_{10} = 3.67$, vs non-dyskinetic, $t_{11} = 4.071$, vs dyskinetic, $\#P < .05$, $\#\#P < .01$, unpaired Student's t test). **(C)** Histogram of the different time to onset of SSD in sham-operated rats and in 6-OHDA rats treated with L-dopa for 3 or 15 days (dyskinetic and non-dyskinetic; sham vs dyskinetic, $t_{25} = 5.32$, $***P < .001$; non-dyskinetic vs dyskinetic, $t_{19} = 3.22$, $**P < .01$, unpaired Student's t test). **(D)** TH-immunostaining in coronal section of the substantia nigra pars compacta (SNc) region of dyskinetic and non-dyskinetic 6-OHDA-lesioned rats treated with L-dopa (2x objective, scale bar 500 μm). **(E)** The graph shows the massive loss of dopaminergic neurons in ipsilateral SNc compared with the contralateral side ($****P = .0001$) both in dyskinetic and non-dyskinetic 6-OHDA-lesioned rats. Ipsi, ipsilateral; contra, contralateral. [Color figure can be viewed at wileyonlinelibrary.com]

induced a significant increase in DA content when compared with the parkinsonian-untreated group ($P < .05$, $P < .01$). In these different groups, we observed that the time to onset of SSD was not the same (Fig. 5C). In fact, in slices from the 6-OHDA dyskinetic rats, SSD appeared significantly earlier ($n = 14$, 1.93 ± 0.10 minutes) than in the sham-operated rats ($n = 13$, 3.43 ± 0.26 minutes, $P < .001$). Time to onset in 3-day-treated rats and non-dyskinetic animals was not

significantly different (6-OHDA plus L-dopa 3 days vs non-dyskinetic, $P > .05$; Fig. 5C). Interestingly, the comparison between the non-dyskinetic versus the dyskinetic group revealed a significant difference in terms of SSD time of onset ($P < .01$). Stereological count of dopaminergic neurons showed that there were no differences in the extent of lesion between the dyskinetic and non-dyskinetic 6-OHDA-lesioned rats, whereas the lesion between ipsi- and contra-lateral sides is confirmed in

both groups (Fig. 5D,E). Taken together, these findings indicate that, although DA replacement treatment restores SSD in the majority of the slices obtained from denervated animals, the slices obtained from dyskinetic rats are significantly more susceptible to initiate SSD than slices from non dyskinetic animals.

Discussion

Main Findings

In the present study, we obtained 2 main novel findings. First, we observed that SSD depends on the concomitant activation of D1-like DA and NMDA receptors, and it is reduced in an experimental model of PD. Second, we found that chronic L-dopa treatment in a rodent model of PD, at a dose inducing dyskinesia, increases the occurrence and speed of propagation of SSD, which in turn has a direct impact on the principal signaling pathway associated to the activation of D1-like receptors.

Role of Glutamate and DA

SD has been postulated to be a main pathophysiological event in various neurological disorders such as migraine, stroke, and traumatic brain injury.³ In experimental animal models and in human brain pathologies, CSD has been widely investigated, and this event has been coupled with diffuse but transient alterations of ion homeostasis, metabolism, and blood flow. Conversely, subcortical forms of SD have been poorly investigated and, although a few reports^{2,30} suggested the existence of SSD, the mechanisms underlying this phenomenon and their pathophysiological relevance are still unknown. In the present study, we found that the striatum, a brain structure deeply involved in motor control as well as in the pathophysiology of movement disorders,¹³ shows reproducible episodes of SSD in response to repetitive increases of extracellular potassium concentration. The occurrence of SSD episodes increases on removal of the magnesium block from NMDA receptors, indicating that SSD relies more on the activation of NMDA rather than AMPA glutamate receptors. Accordingly, in this condition, SSD is blocked by L-APV, but not by CNQX. Interestingly, the experiments in the decorticated slices clearly show that striatal SD is a local striatal feature that could be observed even in this condition by combining imaging and electrophysiological recordings. Moreover, the fact that the NMDA receptor antagonist L-APV significantly reduced SSD in decorticated slices clearly indicates that NMDA receptors, causally implicated in this phenomenon, are located within the striatum. In fact, residual glutamatergic terminals within the slice preparation might release glutamate activating postsynaptic NMDA receptors in striatal neurons. Similarly, the

experiments using tetrodotoxin show that blockage of synaptic transmission is able to significantly reduce SSD amplitude as detected in both imaging and electrophysiological experiments.

Last, a new experimental approach combining the IOS measurements with the amperometric detection of DA changes allowed us to demonstrate that SSD is coupled with increased release of this transmitter. We also found that activation of distinct DA receptors differentially influences the induction of this phenomenon. In fact, SSD is blocked by the D1 receptor antagonist SCH 23390, but not by the D2 receptor antagonist L-sulpiride. Consistent with our pharmacological analysis, we also discovered that the DA denervation, obtained by unilateral injection of 6-OHDA, abolished SSD as well as the peak of DA released during this event measured by amperometry. This finding further supports a key role of endogenous DA in the induction of this phenomenon. However, in DA-denervated slices, SSD could be partially restored in the presence of the D1 receptor agonist SKF 38393.

The functional association between SSD and NMDA receptors found in our studies is consistent with the “glutamate hypothesis,”¹⁰ which suggests that this phenomenon is triggered by an intensive release of glutamate that activates postsynaptic NMDA receptors,³¹ thus evoking further neuronal firing and glutamate release.

Downstream Signaling Pathways

Previous studies have showed that SD causes an increase of both extracellular glutamate and intracellular calcium levels in different brain areas, such as neocortex, hippocampus, and thalamus^{2,32-34} and in turn leads to a transient ERK signaling activation.²⁴ Interestingly, in the present work we demonstrated that SSD is able to induce an increase of the ERK1/2 phosphorylation state in rat striatal slices, suggesting a common molecular substrate in different brain regions, where such a phenomenon takes place. Although in resting cells the intracellular machinery associated to ERK1/2 cascade is mainly localized in the cytoplasm,³⁵ upon stimulation, ERK1/2 rapidly translocates from cytoplasm to the nucleus, where it modulates the activation of the transcription factors necessary for gene expression.^{36,37} In this respect, the immediate early gene *c-Fos* represents one of the main ERK1/2-dependent transcriptional targets under CSD occurrence.^{38,39} Accordingly, in our experimental setting, we were able to find a 10-fold increase of *c-Fos* mRNA expression levels in rat striatal slices showing SSD, thus strengthening the hypothesis that this phenomenon affects different subcellular compartments, ranging from synaptic milieu to nuclear chromatin remodeling. In this respect, different studies showed that ERK signaling modulates *c-Fos* transcriptional activity by phosphorylating the H3 histone at its promoter.^{40,41} In particular,

phosphorylation of H3 at Ser10 residue can trigger chromatin structure rearrangements, turning it into decondensed euchromatin.⁴² Based on these findings, we found for the first time a higher ERK-dependent transcript level of histone H3 phosphorylation at Ser10 residue in the striatal slices displaying the SSD phenomenon. Moreover, we also found a dramatic increase in the mRNA levels of the transcription factor *Npas4*, a neuron-specific activity-dependent gene, the expression of which has been shown to be turned on by the CSD,²⁸ in the rat striatal slices showing SSD when compared with controls.

The striatum is one of the main subcortical entry stations of the basal ganglia involved in the control of motor balance and reward-based learning,⁴³ composed of 90% to 95% of gamma-AminoButyric acid SPNs that express 2 distinct classes of DA receptors, namely, D1-positive SPNs and D2-positive SPNs.⁴⁴ SPNs receive excitatory glutamatergic inputs from the cortex and thalamus, which contact dendritic spines and are modulated by DA released from the terminals of midbrain DA cells. Therefore, we addressed the question of whether, besides glutamate, DA is also able to modulate the onset and propagation of SSD. Together with our optical data, displaying a relevant involvement of D1 DA receptors in the onset and diffusion of SSD, we sought to investigate a potential influence of such a phenomenon on the striatal D1 receptor-mediated signaling. To this aim, we found robust striatal cAMP/PKA activity in the striatal slices showing SSD evaluated through the phosphorylation levels of the AMPA glutamate receptor GluA1 at Ser845. Interestingly, we found that this effect, at least in part, is associated with D1 receptor-dependent activity because it is blocked by the selective D1 receptor antagonist SCH 23390. Consistent with a main role of D1 receptor-dependent signaling in regulating SSD, we also showed that bath-applied SKF 38393 in 6-OHDA-denervated striatal slices normalized the occurrence of this phenomenon and in turn increased the cAMP/PKA activity found altered in DA-denervated slices.

Functional Implications for PD and L-Dopa-Induced Dyskinesia

Because unilateral striatal DA denervation is considered a reliable rodent model of PD, we postulated a scenario in which in experimental parkinsonism the lack of endogenous DA would lower the possible occurrence of SSD, and we predicted that subchronic administration of L-dopa, the gold-standard therapy in PD patients,⁴⁵ should restore SSD. In accordance with our prediction, after subchronic treatment with L-dopa, the percentage of DA-denervated slices showing SSD was similar to that observed in slices from sham-operated animals. This observation indicates that not only the acute activation of D1 receptors by the in vitro

application of a selective agonist but also an in vivo subchronic treatment with L-dopa mimicking a clinical setting in PD patients restores striatal SD. Long-term treatment with L-dopa induces dyskinesia, a disabling condition involving involuntary dystonic and choreic movements.^{46,47} L-dopa-induced dyskinesia (LID) is triggered by an abnormal activation of the D1 DA receptors located on SPNs, leading to gene expression through sequential activation of PKA, dopamine- and cAMP-regulated neuronal phosphoprotein (DARPP-32), ERK, mitogen, and phosphorylation of histone H3 at serine 10.⁴⁸⁻⁵⁰ The speed of onset of SSD and the occurrence of this phenomenon in single slices were significantly higher in animals showing abnormal involuntary movements in comparison with those that did not show a dyskinetic-like behavior. This finding suggests a functional link between SSD and LID. It is interesting to note that in the 6-OHDA rat model of PD, previous experimental work has suggested that even subchronic (3 days) injection with L-dopa can induce dyskinetic-like behavior in a subgroup of animals.⁵¹ However, a longer period of L-dopa treatment (2 weeks) causes LID in a significantly larger proportion of treated animals. This observation may account for our difference in SD expression and propagation in these 2 groups of animals. Nevertheless, the degree of D1 DA receptor sensitivity induced by a prolonged treatment with L-dopa might contribute to the observed increased induction and propagation of SD in animals exposed to a longer treatment.

Surprisingly, however, there was no correlation among groups between the onset of SSD and the release of DA indicating that, although presynaptic mechanisms significantly contribute to dyskinesia,⁵² in our ex vivo experimental condition they do not seem to play a major role.

PD is considered a chronic neurodegenerative condition, whereas SD has been mainly observed in acute neurological conditions such as epilepsy and migraine. However, we would like to stress that in the advanced stage of PD, rather abrupt motor shifts from the on state to the off state can be observed. Moreover, clinical evidence clearly show that PD patients can rapidly fluctuate from a non dyskinetic to a dyskinetic state in a time window of a few minutes. In this scenario, the observed susceptibility to SSD induction could represent a marker of the dyskinetic state or, more intriguingly, its pathophysiological base.

Limitations and Future Perspectives

To get insights into the time course of SSD, we analyzed the response of single SPNs during the SD phenomenon, measuring membrane potential changes by patch-clamp experiments following the application of 26 mM KCl. In this condition, we found that about

1 minute after the onset of KCl application, SPNs membrane potential depolarized, leading to brief firing of action potentials followed by a silencing of action potentials and a prolonged depolarizing state lasting for several minutes (Fig. 1). Moreover, we performed experiments to characterize the changes of extracellular DC potentials in slices following the application of KCl.

Time-course comparisons among the membrane changes recorded in single SPNs and shifts in DC potential as well as modifications of optical signals showed that the SD phenomenon occurred several minutes after the depolarization of single striatal neurons and closely mimicked the time course of IOS changes. These findings taken together seem to indicate that the membrane depolarization/firing inhibition represents early electrical events preceding and possibly triggering the subsequent, long-lasting, SD as observed in optical and DC shift experiments.

Last, as a future perspective, it could be of interest to study the role of glial cells in modulating striatal SD expression. In fact, during PD, inflammatory features have been found to be coupled with changes in astrocytes and microglia after long-term L-dopa treatment. Thus, inflammation and abnormal glial function may play a crucial role in PD and LID induction progression.⁵³ Similarly, it has been reported that glial activity is of critical importance during SD. In fact, SD causes a considerable perturbation of the ionic environment in the brain, which may be readily detected by microglia and other nonneuronal cell types. It is conceivable that inflammation and microglial activation induced by PD-related processes, long-term L-dopa treatment, and repetitive inductions of striatal SD might trigger a vicious circle in the pathophysiology of basal ganglia and in LID induction and maintenance.⁵⁴ ■

Acknowledgments: This work was supported by grants from Progetto di Ricerca di Interesse Nazionale 2011 (prot. 2010AHHP5H to P.C.), Fondazione Cariplo, grant no. 2014-0660 (to P.C.), the Italian Ministry of Health, Ricerca Finalizzata (RF-2013-02357386 to A.U. and A.T. and RF-2013-02356215 to P.C.). This work/project was supported by a grant (V.G., P.C.) from the Fresco Parkinson Institute to New York University School of Medicine and The Marlene and Paolo Fresco Institute for Parkinson's and Movement Disorders, which was made possible with support from Marlene and Paolo Fresco. We thank Regione Umbria for supporting a Ph.D. fellowship to A.M.

References

1. Leao AA, Morrison RS. Propagation of spreading cortical depression. *J Neurophysiol* 1945;8:33-45.
2. Eikermann-Haerter K, Yuzawa I, Qin T, et al. Enhanced subcortical spreading depression in familial hemiplegic migraine type 1 mutant mice. *J Neurosci* 2011;31(15):5755-5763.
3. Ayata C, Lauritzen M. Spreading depression, spreading depolarizations, and the cerebral vasculature. *Physiol Rev* 2015;95(3):953-993.
4. Pietrobon D, Moskowitz MA. Chaos and commotion in the wake of cortical spreading depression and spreading depolarizations. *Nat Rev Neurosci* 2014;15(6):379-393.
5. Mayevsky A, Doron A, Manor T, Meilin S, Zarchin N, Ouaknine GE. Cortical spreading depression recorded from the human brain using a multiparametric monitoring system. *Brain Res* 1996;740(1-2):268-274.
6. Seghatoleslam M, Ghadiri MK, Ghaffarian N, Speckmann EJ, Gorji A. Cortical spreading depression modulates the caudate nucleus activity. *Neuroscience* 2014;267:83-90.
7. Yavich L, Ylinen A. Spreading depression in the cortex differently modulates dopamine release in rat mesolimbic and nigrostriatal terminal fields. *Exp Neurol* 2005;196(1):47-53.
8. Haghiri H, Kovac S, Speckmann EJ, Zilles K, Gorji A. Patterns of neurotransmitter receptor distributions following cortical spreading depression. *Neuroscience* 2009;163(4):1340-1352.
9. Aiba I, Shuttleworth CW. Sustained NMDA receptor activation by spreading depolarizations can initiate excitotoxic injury in metabolically compromised neurons. *J Physiol* 2012;590(22):5877-5893.
10. Shatillo A, Salo RA, Giniatullin R, Grohn OH. Involvement of NMDA receptor subtypes in cortical spreading depression in rats assessed by fMRI. *Neuropharmacology* 2015;93:164-170.
11. Tozzi A, de Iure A, Di Filippo M, et al. Critical role of calcitonin gene-related peptide receptors in cortical spreading depression. *Proc Natl Acad Sci U S A* 2012;109(46):18985-18990.
12. Moghaddam B, Gruen RJ, Roth RH, Bunney BS, Adams RN. Effect of L-glutamate on the release of striatal dopamine: in vivo dialysis and electrochemical studies. *Brain Res* 1990;518(1-2):55-60.
13. Calabresi P, Picconi B, Tozzi A, Ghiglieri V, Di Filippo M. Direct and indirect pathways of basal ganglia: a critical reappraisal. *Nat Neurosci* 2014;17(8):1022-1030.
14. Suarez LM, Alberquilla S, Garcia-Montes JR, Moratalla R. Differential synaptic remodeling by dopamine in direct and indirect striatal projection neurons in *Pitx3(-/-)* mice, a genetic model of Parkinson's disease. *J Neurosci* 2018;38(15):3619-3630.
15. Suarez LM, Solis O, Aguado C, Lujan R, Moratalla R. L-DOPA oppositely regulates synaptic strength and spine morphology in D1 and D2 striatal projection neurons in dyskinesia. *Cereb Cortex* 2016;26(11):4253-4264.
16. Picconi B, Centonze D, Hakansson K, et al. Loss of bidirectional striatal synaptic plasticity in L-DOPA-induced dyskinesia. *Nat Neurosci* 2003;6(5):501-506.
17. Napolitano F, Bonito-Oliva A, Federici M, et al. Role of aberrant striatal dopamine D1 receptor/cAMP/protein kinase A/DARPP32 signaling in the paradoxical calming effect of amphetamine. *J Neurosci* 2010;30(33):11043-11056.
18. Picconi B, Ghiglieri V, Bagezza V, Barone I, Sgobio C, Calabresi P. Striatal synaptic changes in experimental parkinsonism: role of NMDA receptor trafficking in PSD. *Parkinsonism Relat Disord* 2008;14(suppl 2):S145-S149.
19. Cenci MA, Lee CS, Bjorklund A. L-DOPA-induced dyskinesia in the rat is associated with striatal overexpression of prodynorphin- and glutamic acid decarboxylase mRNA. *Eur J Neurosci* 1998;10(8):2694-2706.
20. Santini E, Alcacer C, Cacciatore S, et al. L-DOPA activates ERK signaling and phosphorylates histone H3 in the striatonigral medium spiny neurons of hemiparkinsonian mice. *J Neurochem* 2009;108(3):621-633.
21. Andrew RD, Jarvis CR, Obeidat AS. Potential sources of intrinsic optical signals imaged in live brain slices. *Methods* 1999;18(2):185-196, 179.
22. Torrente D, Mendes-da-Silva RF, Lopes AA, Gonzalez J, Barreto GE, Guedes RC. Increased calcium influx triggers and accelerates cortical spreading depression in vivo in male adult rats. *Neurosci Lett* 2014;558:87-90.
23. Krapivinsky G, Krapivinsky L, Manasian Y, et al. The NMDA receptor is coupled to the ERK pathway by a direct interaction between NR2B and RasGRF1. *Neuron* 2003;40(4):775-784.
24. Chow AK, Thompson CS, Hogan MJ, Banner D, Sabourin LA, Hakim AM. Cortical spreading depression transiently activates MAP kinases. *Brain Res Mol Brain Res* 2002;99(1):75-81.
25. Keibabian JW, Calne DB. Multiple receptors for dopamine. *Nature* 1979;277(5692):93-96.

26. Corvol JC, Studler JM, Schonn JS, Girault JA, Herve D. Alpha(olf) is necessary for coupling D1 and A2a receptors to adenylyl cyclase in the striatum. *J Neurochem* 2001;76(5):1585-1588.

27. Roche KW, O'Brien RJ, Mammen AL, Bernhardt J, Haganir RL. Characterization of multiple phosphorylation sites on the AMPA receptor GluR1 subunit. *Neuron* 1996;16(6):1179-1188.

28. Yoshida K, Xu M, Natsubori A, Mimura M, Takata N, Tanaka KF. Identification of the extent of cortical spreading depression propagation by Npas4 mRNA expression. *Neurosci Res* 2015;98:1-8.

29. Bastide MF, Meissner WG, Picconi B, et al. Pathophysiology of L-dopa-induced motor and non-motor complications in Parkinson's disease. *Prog Neurobiol* 2015;132:96-168.

30. Kasser RJ, Renner KJ, Feng JX, Brazell MP, Adams RN. Spreading depression induced by 100 mM KCl in caudate is blocked by local anesthesia of the substantia nigra. *Brain Res* 1988;475(2):333-344.

31. Pietrobon D, Moskowitz MA. Pathophysiology of migraine. *Annu Rev Physiol* 2013;75:365-391.

32. Basarsky TA, Feighan D, MacVicar BA. Glutamate release through volume-activated channels during spreading depression. *J Neurosci* 1999;19(15):6439-6445.

33. Gniel HM, Martin RL. Changes in membrane potential and the intracellular calcium concentration during CSD and OGD in layer V and layer II/III mouse cortical neurons. *J Neurophysiol* 2010;104(6):3203-3212.

34. Rosen LB, Ginty DD, Weber MJ, Greenberg ME. Membrane depolarization and calcium influx stimulate MEK and MAP kinase via activation of Ras. *Neuron* 1994;12(6):1207-1221.

35. Yao Z, Seger R. The ERK signaling cascade—views from different subcellular compartments. *Biofactors* 2009;35(5):407-416.

36. Chen RH, Sarnecki C, Blenis J. Nuclear localization and regulation of erk- and rsk-encoded protein kinases. *Mol Cell Biol* 1992;12(3):915-927.

37. Plotnikov A, Zehorai E, Procaccia S, Seger R. The MAPK cascades: signaling components, nuclear roles and mechanisms of nuclear translocation. *Biochim Biophys Acta* 2011;1813(9):1619-1633.

38. Herrera DG, Robertson HA. Application of potassium chloride to the brain surface induces the c-fos proto-oncogene: reversal by MK-801. *Brain Res* 1990;510(1):166-170.

39. Moskowitz MA, Nozaki K, Kraig RP. Neocortical spreading depression provokes the expression of c-fos protein-like immunoreactivity within trigeminal nucleus caudalis via trigeminovascular mechanisms. *J Neurosci* 1993;13(3):1167-1177.

40. Brami-Cherrier K, Roze E, Girault JA, Betuing S, Caboche J. Role of the ERK/MSK1 signalling pathway in chromatin remodelling and brain responses to drugs of abuse. *J Neurochem* 2009;108(6):1323-1335.

41. Thomson S, Clayton AL, Hazzalin CA, Rose S, Barratt MJ, Mahadevan LC. The nucleosomal response associated with immediate-early gene induction is mediated via alternative MAP kinase cascades: MSK1 as a potential histone H3/HMG-14 kinase. *EMBO J* 1999;18(17):4779-4793.

42. Bao X, Cai W, Deng H, et al. The COOH-terminal domain of the JIL-1 histone H3S10 kinase interacts with histone H3 and is required for correct targeting to chromatin. *J Biol Chem* 2008;283(47):32741-32750.

43. Graybiel AM. Neurotransmitters and neuromodulators in the basal ganglia. *Trends Neurosci* 1990;13(7):244-254.

44. Bertran-Gonzalez J, Herve D, Girault JA, Valjent E. What is the degree of segregation between striatonigral and striatopallidal projections? *Front Neuroanat* 2010;4:136.

45. Olanow CW, Lees A, Obeso J. Levodopa therapy for Parkinson's disease: challenges and future prospects. *Mov Disord* 2008;23(suppl 3):S495-S496.

46. Calabresi P, Di Filippo M, Ghiglieri V, Tambasco N, Picconi B. Levodopa-induced dyskinesias in patients with Parkinson's disease: filling the bench-to bedside gap. *Lancet Neurol* 2010;9(11):1106-1117.

47. Obeso JA, Merello M, Rodriguez-Oroz MC, Marin C, Guridi J, Alvarez L. Levodopa-induced dyskinesias in Parkinson's disease. *Handb Clin Neurol* 2007;84:185-218.

48. Darmopil S, Martin AB, De Diego IR, Ares S, Moratalla R. Genetic inactivation of dopamine D1 but not D2 receptors inhibits L-DOPA-induced dyskinesia and histone activation. *Biol Psychiatry* 2009;66(6):603-613.

49. Lebel M, Chagniel L, Bureau G, Cyr M. Striatal inhibition of PKA prevents levodopa-induced behavioural and molecular changes in the hemiparkinsonian rat. *Neurobiol Dis* 2010;38(1):59-67.

50. Santini E, Feyder M, Gangarossa G, Bateup HS, Greengard P, Fisone G. Dopamine- and cAMP-regulated phosphoprotein of 32-kDa (DARPP-32)-dependent activation of extracellular signal-regulated kinase (ERK) and mammalian target of rapamycin complex 1 (mTORC1) signaling in experimental parkinsonism. *J Biol Chem* 2012;287(33):27806-27812.

51. Winkler C, Kirik D, Bjorklund A, Cenci MA. L-DOPA-induced dyskinesia in the intrastriatal 6-hydroxydopamine model of parkinson's disease: relation to motor and cellular parameters of nigrostriatal function. *Neurobiol Dis* 2002;10(2):165-186.

52. Cenci MA. Presynaptic mechanisms of L-DOPA-induced dyskinesia: the findings, the debate, and the therapeutic implications. *Front Neurol* 2014;5:242.

53. Del-Bel E, Bortolanza M, Dos-Santos-Pereira M, Bariotto K, Raisman-Vozari R. L-DOPA-induced dyskinesia in Parkinson's disease: are neuroinflammation and astrocytes key elements? *Synapse* 2016;70(12):479-500.

54. Shibata M, Suzuki N. Exploring the role of microglia in cortical spreading depression in neurological disease. *J Cereb Blood Flow Metab* 2017;37(4):1182-1191.

55. Gardoni F, Picconi B, Ghiglieri V, et al. A critical interaction between NR2B and MAGUK in L-DOPA induced dyskinesia. *J Neurosci* 2006;26(11):2914-2922.

56. Paxinos G, Charles W. *The Rat Brain in Stereotaxic Coordinates*. 5th ed. New York: Academic Press; 2005.

Supporting Data

Additional Supporting Information may be found in the online version of this article at the publisher's web-site.